



MINISTRY OF AVIATION

AERONAUTICAL RESEARCH COUNCIL
REPORTS AND MEMORANDA

Some Tests on High-Reaction Compressor Blading

By R. C. TURNER and R. A. BURROWS

LONDON: HER MAJESTY'S STATIONERY OFFICE

1964

PRICE 8s. 6d. NET

Some Tests on High-Reaction Compressor Blading

By R. C. TURNER and R. A. BURROWS

COMMUNICATED BY THE DEPUTY CONTROLLER AIRCRAFT (RESEARCH AND DEVELOPMENT),
MINISTRY OF AVIATION

*Reports and Memoranda No. 3380**
January, 1963

Summary.

Two sets of blading, designed for 120 per cent reaction, and for flow coefficients of 0·667 and 1·0 respectively, have been tested in the N.G.T.E. low-speed compressor No. 106. The performances were compared with those of corresponding sets of 50-per-cent-reaction blading and with predictions based on simple theoretical methods.

The high-reaction bladings both gave efficiencies which were lower by amounts broadly in line with the predictions. The work-done factors were also appreciably lower.

The lower-flow-coefficient blading showed a significant advantage in pressure rise over its 50-per-cent-reaction counterpart, with about the same surge flow, while the high-flow blading was deficient in pressure rise but had a considerably wider surge margin. Both bladings might thus be of value in specialised situations where efficiency is not a prime consideration.

LIST OF CONTENTS

Section

1. Introduction
2. The Compressor
3. The Blading
4. Measurements
5. Test Results
6. Discussion
7. Conclusions

Notation

References

Appendices I to V

Illustrations—Figs. 1 to 9

Detachable Abstract Cards

* Replaces N.G.T.E. Report No. R.252—A.R.C. 24 568.

LIST OF APPENDICES

Appendix

- I. Design details of M120 blading
- II. Design details of H120 blading
- III. Design details of M50 blading
- IV. Design details of H50 blading
- V. Note on the calculation of the parameters

LIST OF ILLUSTRATIONS

Figure

1. Assembly of compressor
2. Overall characteristics. M120 and M50 bladings
3. Stage characteristics. M120 and M50 bladings
4. Test and theoretical overall characteristics compared. M120 and M50 bladings
5. Overall characteristics. H120 and H50 bladings
6. Stage characteristics. H120 and H50 bladings
7. Test and theoretical overall characteristics compared. H120 and H50 bladings
8. Comparisons of torque and thermocouple efficiencies. All bladings
9. Outlet-annulus velocity profiles. All bladings

1. Introduction.

In the design of axial compressors, it is usually considered desirable to keep the number of stages to a minimum. This is especially so in machines intended for use with light gases, e.g. helium, where the high specific heats result in relatively low stage temperature rises and hence relatively large numbers of stages for a given overall compression temperature rise.

One possible method of increasing the stage temperature rise is the use of high degrees of reaction. This is discussed in Ref. 1. In Britain, most compressor designs are not very far removed from 50 per cent reaction at the mean diameter. There is little published work on high-reaction blading; some test results for low- and medium-flow-coefficient designs are however given in Ref. 2.

One of the chief objections to high-reaction designs is their lower theoretical efficiency; Refs. 1 and 3 present curves which illustrate the drop as the reaction is increased above 50 per cent. Another is that the gas velocities relative to the rotor blades reach high values. This could result in Mach number troubles in air compressors; for light gases, however, the sonic velocities are generally sufficiently high to preclude the occurrence of supercritical Mach numbers at the maximum blade speeds that stress limitations will allow.

On the credit side it has sometimes been suggested that the accelerating passages of the stator rows of compressors of more than 100 per cent reaction might result in more uniform velocity profiles across the annulus. The work-done factors might therefore be higher, thus increasing the already theoretically high temperature rise. Also, the secondary losses might be lower, with a consequent increase in efficiency above the rather low value predicted by simple theory.

It was evident that reliable experimental information was required before the value of high-reaction designs could be assessed. Accordingly, two sets of blading were designed for 120 per cent reaction, at flow coefficients of 0.667 and 1.0 respectively, for testing in a six-stage build of the N.G.T.E. '106' low-speed compressor. These values of flow coefficient were thought to cover certain possible practical applications; Ref. 1 shows that the theoretical advantage of high reaction is in fact more marked at the lower values. To provide a basis of comparison, corresponding sets of 50-per-cent-reaction blading were also manufactured. For convenience, the two sets of 120-per-cent-reaction blading are referred to as M120 and H120 respectively, while the corresponding sets of 50-per-cent-reaction blading are referred to as M50 and H50; M and H indicate 'medium' and 'high' flow coefficients respectively.

Data relating to the tests on the H120 and H50 bladings have already been published in a preliminary report⁴, but are repeated here in full.

2. *The Compressor.*

The 106 compressor is described in Ref. 5. It is a low-speed machine of constant annulus dimensions, assembled for the present tests with six stages. Fig. 1 shows a general arrangement. At the normal running speed of 3000 rev/min, the Reynolds number based on the blade speed and chord at the mean diameter is 1.3×10^5 . The change in density across the compressor is small, so all the stages work at nearly the same flow coefficient at all running conditions.

3. *The Blading.*

The M120 and H120 bladings were designed on conventional lines as far as possible, so that the degree of reaction was the only unusual feature. Reaction was taken to be the ratio of the static-temperature rise across a rotor blade row to that across the complete stage. A value of 120 per cent was chosen at the mean diameter, with rotor air deflections as given by Ref. 3 at mean-diameter flow coefficients of 0.667 and 1.0 respectively. At other blade heights, the air angles were based on free-vortex twist. Both rotor and stator blades were of constant chord, the blade angles being calculated on the assumption of zero incidence and with the deviation rules of Ref. 6. C4 sections on circular-arc camber lines were used throughout. It would of course have been possible to design the stator blades using conventional turbine methods as outlined for instance in Ref. 7, but it was considered that little advantage would be gained, and in any case it was desired to use conventional 'compressor' methods as far as possible. Full details of the bladings are given in Appendices I and II respectively.

The M50 and H50 bladings were designed on generally similar lines and at corresponding flow coefficients, the main difference being that the reaction at mean diameter was 50 per cent in both cases. The M50 blading differed slightly from the other designs in thickness and pitch/chord ratio away from the mean diameter, and the design incidence was not quite zero. It had been originally designed for another purpose, but it is not thought that these differences are significant in the present context. Details of the M50 and H50 bladings are given in Appendices III and IV respectively.

In all the builds, the sixth stage was identical with the others, this arrangement being considered the best for research purposes. In a compressor for a particular application, however, steps would usually be taken to remove the swirl after the last stage where this exceeded about 10° , as in the M120, M50, and H120 bladings. This would necessitate modified last-stage stator blades, or an additional row of outlet guide blades in the M50 blading. In the M120 and H120 bladings, however,

it might well be sufficient to remove the last stator blades altogether, since the mean-diameter swirl after the rotor blades was under 10° in both cases at the design condition.

4. Measurements.

Input torque was estimated from the reaction on the casing of the driving motor; an arbitrary allowance was made for the compressor bearing torque by measurement of the input torque at a series of very low speeds and extrapolation to zero speed. Mass flow was measured by means of a standard orifice in the delivery ducting. The inlet total pressure was taken as atmospheric, the loss across the inlet gauze being neglected. The outlet total pressure was derived from two five-point pitot combs spaced 180° apart in the outlet annulus, two chords downstream of the last-stage stator blades. The pitot points were spaced equally across the annulus, and corresponding points of the two combs were connected *via* a manifold to the same manometer. The outlet total pressure was taken as the arithmetic mean of the five readings. In addition, there were four static tappings after each stage; these were connected to a single manometer *via* a manifold.

In order to provide a check on the efficiency, thermocouples were used in some tests to measure the total-temperature rise directly. Six chromel-constantan thermocouples at the inlet were connected in series with six in the outlet ducting, conventional stagnation sheaths being used.

5. Test Results.

Appendix V gives the methods of calculation of the leading parameters. The overall characteristics for the M120 and M50 bladings are shown in Fig. 2, two test runs having been made for each blading. They are based on the overall total-pressure and total-temperature rises divided by the number of stages, and are in effect mean stage characteristics. The individual stage characteristics, showing pressure rise only, are calculated from the stage static-pressure rises and are given in Fig. 3. It is not practicable in this compressor to measure individual stage temperature rises. Fig. 4 compares the test overall characteristics with the theoretical stage characteristics which, strictly speaking, refer to rather higher Reynolds numbers than those of the tests. In the calculation of the theoretical characteristics of the M120 blading, the data of Ref. 3 and the design-point deviation rule of Ref. 6 were used for the rotor blades, and the data and deviation rules of Ref. 8 for the stator blades, the latter being effectively a turbine blade row. For the M50 blading, the data of Ref. 3 with the design-point deviation rule of Ref. 6 were used throughout. A work-done factor of 0.8 has been used in plotting the theoretical characteristics of both bladings. This is merely a convenient figure which brings the characteristics very roughly to the same level as the test characteristics, and thus assists presentation of the curves; the theoretical efficiency curves are of course independent of the assumed work-done factor. It should, however, be remembered that its value will influence the slopes as well as the levels of the temperature- and pressure-rise characteristics.

Figs. 5, 6 and 7 relate to the H120 and H50 bladings and correspond to Figs. 2, 3 and 4.

Fig. 8 shows the results of some tests where efficiencies were derived from direct temperature measurement by means of thermocouples as well as from the torque and mass-flow readings. The H120 and H50 bladings were run at 2500 rev/min for these particular tests; it is not thought that the results would have been significantly different at 3000 rev/min.

Fig. 9 presents outlet velocity profiles for all the bladings. The velocities were calculated from the readings of the outlet pitot combs and the local wall static pressures; it was assumed that the swirl was that given by the stator design air outlet angles at any position. The mean axial velocities

used in the calculation of V_a/\bar{V}_a were derived from integration of the profiles. Three profiles are given for each blading; they refer respectively to conditions near surge, near the design flow coefficient, and near the highest flow coefficient of the test runs.

6. Discussion.

Test results obtained from this compressor can be regarded as comparative only; the blading Reynolds number is rather low, and the derived temperature-rise measurements based on the torque are also probably rendered somewhat inaccurate by the compressor bearing friction and rotor windage which is difficult to estimate under running conditions. They are also subject to any errors in the mass-flow measurement. As the overall temperature rises are somewhat low (about 10°C and 18°C for the M50 and H120 bladings respectively at the design flows) it is not easy to measure them directly, especially as the inlet air (inspired directly from the laboratory) is subject to small fluctuations of temperature. Nevertheless, the directly measured temperature rises based on the thermocouple readings probably give on average a better absolute measure of compressor efficiency. On the other hand, Fig. 8 shows that the differences between the directly measured temperature rises and the derived values in the various tests are reasonably consistent, and in addition the latter exhibit less general scatter. The authors have therefore preferred to base their comparative analyses between the various builds upon the derived values of temperature rise.

Reference to Figs. 2 and 4 for the medium-flow-coefficient bladings and to Figs. 5 and 7 for the high-flow-coefficient bladings shows that there is a broad general correspondence between the test and theoretical characteristics, although there are considerable differences of detail. The following table compares the leading parameters of all the bladings:

Blading	M120	M50	H120	H50
Design $\frac{\bar{V}_a}{U}$	0.667	0.667	1.00	1.00
Reaction % at design $\frac{\bar{V}_a}{U}$	120	50	120	50
$\eta \left(\text{design } \frac{\bar{V}_a}{U} \right)$	0.755	0.829	0.772	0.828
$\eta_{th} \left(\text{design } \frac{\bar{V}_a}{U} \right)$	0.825	0.912	0.832	0.898
$\frac{\eta}{\eta_{th}} \left(\text{design } \frac{\bar{V}_a}{U} \right)$	0.915	0.909	0.928	0.922
$\Omega \left(\text{design } \frac{\bar{V}_a}{U} \right)$	0.778	0.825	0.858	0.912
$\frac{\Delta P}{\frac{1}{2}\rho U^2} \left(\text{design } \frac{\bar{V}_a}{U} \right)$	0.676	0.574	0.943	0.983
$\frac{\bar{V}_a}{U}$ (surge)	0.526	0.530	0.630	0.783
$\frac{\bar{V}_a}{U} \left(\text{peak } \frac{\Delta P}{\frac{1}{2}\rho U^2} \right)$	0.565	—	0.885	0.830
$\frac{\bar{V}_a}{U} \left(\text{peak } \frac{\Delta P}{\frac{1}{2}\rho U^2} \text{ th} \right)$	0.555	0.520	0.895	0.820

The experimental values in this table are derived from the curves drawn through the test points of two test runs, as illustrated in the various figures. The third decimal place is included but in view of the scatter of the test points should not be regarded as necessarily significant.

The close correspondence between the test and theoretical efficiencies is shown by the ratio η/η_{th} which is about 0.91 for both the M120 and the M50 bladings, and 0.93 for both the H120 and the H50 bladings. It is evident that the theoretical values give a good guide to the relative merits of the high-reaction and corresponding 50-per-cent-reaction bladings, so far as efficiency at the design flow coefficient is concerned.

The work-done factors of the high-reaction bladings are significantly lower than those of the corresponding 50-per-cent-reaction bladings, the ratio being 0.94 for both the medium- and the high-flow-coefficient designs. The work-done factor also appears to depend on the design flow coefficient, the ratio of the value for either of the medium-flow-coefficient bladings to that for the corresponding (i.e. same reaction) high-flow-coefficient blading being 0.91. These work-done factors are based on the deviation rules of Ref. 6. If the deviation rules of Ref. 8 had been used for the stator blades of the high-reaction bladings as in the calculation of the theoretical characteristics of Figs. 4 and 7, somewhat lower values would have been obtained for these bladings.

The value of the pressure-rise coefficient depends on the theoretically attainable temperature-rise coefficient as well as on the efficiency and work-done factor. Ref. 1 shows that the advantage of high-reaction designs so far as theoretical temperature rise is concerned becomes greater as the design flow coefficient decreases. It is therefore reasonable to look for the greatest advantage in pressure rise in the M120 blading as compared with the M50 blading. In fact, the M120 blading does show a marked superiority in this respect, by about 18 per cent, in spite of the lower efficiency and work-done factor. The H120 blading, however, is actually inferior in pressure rise to the H50 blading at the design flow; the rather smaller advantage in theoretical temperature rise is here outweighed by the effect of low efficiency and work-done factor.

Examination of the test characteristics shows that the peak value of the pressure-rise coefficient is reached before surge occurs in the M120, H50 and H120 bladings. The surge flows of the M120 and M50 bladings are similar in magnitude, that of the M120 being slightly smaller, but the surge flow of the H120 blading is about 20 per cent lower than that of the H50. This could be an advantage in an application where a wide surge margin was more important than high efficiency, but attention would have to be given to the stability of the system in operational conditions where the compressor was required to work on the wide positive-slope portion of the pressure-rise characteristic. It is unfortunately not possible to judge how the extra surge margin of high-reaction blading would vary with design flow coefficient between the two values of reaction of the present tests.

Surge is not predicted in the theoretical characteristics; it is often arbitrarily taken to occur at the peak of the pressure-rise characteristics, though this is not supported by the present tests. Nevertheless, it is interesting to note that for the three bladings where a peak occurs, the corresponding flow coefficients are close to the theoretical values.

Fig. 9 compares efficiencies based on direct temperature measurement by means of thermocouples with the corresponding values based on the torque readings. The thermocouple efficiencies are consistently higher than the torque values, but show the same trends and do not invalidate the general deductions already made.

Examination of the stage characteristics in Figs. 3 and 6 shows that Stage 1 gives an appreciably different performance from that of the other stages. This is a common experience on the 106

compressor, and suggests that any conclusions derived from the overall performance in the present tests would not be directly applicable to single stages. In the absence of interstage temperature measurement, it is not possible to examine individual stage efficiencies or work-done factors. The general shape of the pressure-rise characteristics may, however, give some indication of stage behaviour; for instance the characteristics of Stages 3 to 6 of the H120 blading in Fig. 6 suggest that partial stalling occurs at flow coefficients below about 0.9.

Fig. 9 presents outlet velocity profiles for all of the bladings. They relate to flow coefficients near the design values, near the surge and near the highest flows of the tests. As they are based on somewhat limited test information, they must be regarded with a certain amount of reserve. The profiles near the design conditions are of most interest in the present context. There is no evidence that the profiles of the high-reaction bladings are significantly more uniform than those of the 50-per-cent-reaction bladings although, compared with the latter, their peaks are situated more towards the outer diameter. In all the bladings except the M50, the flow is displaced towards the outer diameter as surge is approached. This is especially well marked with the H120 blading, and suggests that the partial stalling at lower flows indicated by the stage characteristics occurs towards the inner diameter. It is also interesting to note that in the one blading (M50) where the flow does not appear to move in this way, the overall pressure-rise characteristic does not exhibit a peak before surge occurs.

7. Conclusions.

Two sets of 120-per-cent-reaction blading, designed for flow coefficients of 0.667 and 1.0 respectively, have been tested in the N.G.T.E. '106' compressor, the results being compared with those obtained from corresponding sets of 50-per-cent-reaction blading.

At the design flow coefficients the ratios of measured efficiency to theoretical efficiency for the high-reaction bladings were the same as for the corresponding 50-per-cent-reaction bladings. It is concluded that the theoretical efficiencies provide a satisfactory guide to the relative trends in efficiency to be expected from variation of the design reaction.

The mean work-done factors of the high-reaction bladings were significantly lower than those of the corresponding 50-per-cent-reaction bladings, the high-reaction factor being 0.94 of the corresponding 50-per-cent-reaction factor at the respective design flow coefficients.

The pressure rise of the lower-flow-coefficient high-reaction blading showed a considerable advantage over that of the corresponding 50-per-cent-reaction blading, as predicted theoretically. This could be of value in an application where a reduced efficiency was acceptable. The pressure rise of the high-flow high-reaction blading was generally less than that of the corresponding 50-per-cent-reaction blading. It did, however, have a considerably wider surge margin; this again might be an advantage in a specialised application, although attention to stability of operation would be needed where the pressure-rise characteristic had a positive slope.

At the design condition, the outlet-annulus velocity profiles of the high-reaction bladings showed about the same degree of non-uniformity as their 50-per-cent-reaction counterparts, and there was thus no evidence to suggest that high-reaction designs produce more uniform profiles.

NOTATION

K_p	Specific heat of air at constant pressure
U	Blade speed at mean diameter
V_a	Axial velocity
\bar{V}_a	Mean axial velocity
ΔP	Total- or static-pressure rise per stage
ΔT	Total-temperature rise per stage
c	Blade chord
r	Radius
s	Blade pitch
t	Blade maximum thickness
α	Air angle measured from axial direction
β	Blade angle measured from axial direction
ρ	Air density
η	Isentropic efficiency
Ω	Work-done factor
<i>Suffices</i>	
0	Inlet guide-blade-row outlet
1	Rotor blade-row inlet
2	Rotor blade-row outlet
3	Stator or inlet guide-blade-row inlet
4	Stator blade-row outlet
th	Theoretical

REFERENCES

<i>No.</i>	<i>Author(s)</i>	<i>Title, etc.</i>
1	A. D. S. Carter	An examination of present basic knowledge applied to the design of axial compressors using light gases. A.R.C. 20 212. March, 1958.
2	J. H. Horlock	Axial flow compressors. Fluid mechanics and thermodynamics. Butterworths Scientific Publications. 1958.
3	A. R. Howell	Fluid dynamics of axial compressors. <i>Proc. I. Mech. E.</i> Vol. 153, W.E.P. No. 12. 1945.
4	R. C. Turner and R. A. Burrows ..	A comparison of compressor bladings designed for 120 per cent and 50 per cent reaction at a flow coefficient of 1.0. A.R.C. 21 916. March, 1960.
5	R. A. Jeffs	Description of the low speed experimental compressor No. 106. Power Jets Report R1198. A.R.C. 10 832. April, 1946.
6	A. D. S. Carter	The low speed performance of related aerofoils in cascade. A.R.C. C.P.29. September, 1949.
7	D. G. Ainley and G. C. R. Mathieson	An examination of the flow and pressure losses in blade rows of axial flow turbines. A.R.C. R. & M. 2891. March, 1951.
8	D. G. Ainley and G. C. R. Mathieson	A method of performance estimation for axial flow turbines. A.R.C. R. & M. 2974. December, 1951.

APPENDIX I

Design Details of M120 Blading

The blades were of C4 section on circular-arc camber lines. The blade chord was 1.1 in. at all positions, and there were 58 rotor and 60 stator blades per row. The blade height was 2.5 in., with a mean diameter of 17.5 in.

Rotor blades

r	7.75	8.75	9.75
β_1	65.1	65.9	66.8
β_2	42.8	47.7	51.7
s/c	0.763	0.862	0.961
t/c	0.12	0.10	0.08
α_2	49.5	53.7	57.1

Stator blades

r	7.75	8.75	9.75
β_3	8.9	7.9	7.1
β_4	-48.1	-45.2	-42.7
s/c	0.739	0.833	0.928
t/c	0.10	0.11	0.12
α_4	-39.7	-36.3	-33.4

Inlet guide blades

r	7.75	8.75	9.75
β_3	0	0	0
β_0	-46.5	-43.5	-41.0
s/c	0.739	0.833	0.928
t/c	0.10	0.11	0.12
α_0	-39.7	-36.3	-33.4

APPENDIX II

Design Details of H120 Blading

The blades were of C4 section on circular-arc camber lines. The blade chord was 1.1 in. at all positions and there were 58 rotor and 60 stator blades per row. The blade height was 2.5 in., with a mean diameter of 17.5 in.

Rotor blades

r	7.75	8.75	9.75
β_1	56.6	57.3	58.2
β_2	27.7	33.0	37.7
s/c	0.763	0.862	0.961
t/c	0.12	0.10	0.08
α_2	35.3	40.1	44.2

Stator blades

r	7.75	8.75	9.75
β_3	10.1	9.0	8.1
β_4	-39.6	-37.0	-34.7
s/c	0.739	0.833	0.928
t/c	0.10	0.11	0.12
α_4	-32.2	-29.2	-26.6

Inlet guide blades

r	7.75	8.75	9.75
β_3	0	0	0
β_0	-37.8	-35.1	-32.7
s/c	0.739	0.833	0.928
t/c	0.10	0.11	0.12
α_0	-32.2	-29.2	-26.6

APPENDIX III

Design Details of M50 Blading

The blades were of C4 section on circular-arc camber lines. The blade chords were 1.14, 1.10, and 1.06 in. at root, mean and tip respectively, and there were 58 rotor and 60 stator blades per row. The blade height was 2.5 in., with a mean diameter of 17.5 in.

Rotor blades

r	7.75	8.75	9.75
β_1	40.3	46.5	49.9
β_2	- 1.0	+ 15.6	28.8
s/c	0.739	0.862	0.990
t/c	0.118	0.10	0.084
α_2	8.9	23.4	35.0

Stator blades

r	7.75	8.75	9.75
β_3	50.8	46.1	42.5
β_4	18.1	15.9	14.1
s/c	0.761	0.833	0.899
t/c	0.101	0.11	0.118
α_4	26.1	23.4	21.2

Inlet guide blades

r	7.75	8.75	9.75
β_3	0	0	0
β_0	30.9	28.2	26.1
s/c	0.761	0.833	0.899
t/c	0.101	0.11	0.118
α_0	26.1	23.4	21.2

APPENDIX IV

Design Details of H50 Blading

The blades were of C4 section on circular-arc camber lines. The blade chord was 1.1 in. at all positions, and there were 58 rotor and 60 stator blades per row. The blade height was 2.5 in., with a mean diameter of 17.5 in.

Rotor blades

r	7.75	8.75	9.75
β_1	34.8	39.7	43.9
β_2	-12.4	+ 0.7	12.1
s/c	0.763	0.862	0.961
t/c	0.12	0.10	0.08
α_2	- 3.0	+ 9.6	20.2

Stator blades

r	7.75	8.75	9.75
β_3	43.2	39.7	36.7
β_4	2.0	0.9	0.1
s/c	0.739	0.833	0.928
t/c	0.10	0.11	0.12
α_4	10.8	9.6	8.6

Inlet guide blades

r	7.75	8.75	9.75
β_3	0	0	0
β_0	12.8	11.6	10.7
s/c	0.739	0.833	0.928
t/c	0.10	0.11	0.12
α_0	10.8	9.6	8.6

APPENDIX V

Note on the Calculation of the Parameters

Density ρ .

The mean density of the air was taken as the mean of the atmospheric density and an arbitrary value of the density at the compressor outlet based on the measured total pressure and corresponding isentropic temperature rise. This value was used in the calculation of the overall pressure rise and mean flow coefficients. In the calculation of the individual stage characteristics, the value was adjusted according to the stage number.

Flow Coefficient \bar{V}_a/U .

For the overall characteristics, the mean axial velocity \bar{V}_a was based on the overall mean density and the measured mass flow. For the individual stage characteristics, the density was adjusted according to the stage number. The peripheral blade speed U was taken at the mean diameter for this and for the other coefficients.

Pressure-Rise Coefficient $\Delta P/\frac{1}{2}\rho U^2$.

The density ρ and blade speed U were as defined above. For the overall characteristics (which are effectively mean stage characteristics), the pressure rise ΔP was the measured total-pressure rise, i.e. the excess above atmospheric pressure of the readings of the outlet combs, divided by the number of stages. For the individual stage characteristics, the density was adjusted according to the stage number.

Temperature-Rise Coefficient $K_p \Delta T/\frac{1}{2}U^2$.

The temperature rise ΔT was derived from the input torque, speed, and mass flow. The specific heat of air K_p was in appropriate units so as to render the coefficient non-dimensional. A correction was made for the bearing friction torque which was estimated by the extrapolation to zero speed of the torque values measured at a series of very low speeds. In some of the tests, the temperature rise was measured directly by means of thermocouples.

Isentropic Efficiency η .

The efficiency was calculated from the measured total-pressure rise and the total-temperature rise calculated as above.

Outlet Velocity-Profile Parameter V_a/\bar{V}_a .

This parameter was based on the five pitot readings across the outlet annulus. The outlet estimated total temperature and the outlet outer-diameter static pressure were assumed to apply across the annulus, and the outlet air angles from the last-stage stator blades were taken as the theoretical values. The axial velocity at each of the five positions was integrated graphically to give the mean value \bar{V}_a .

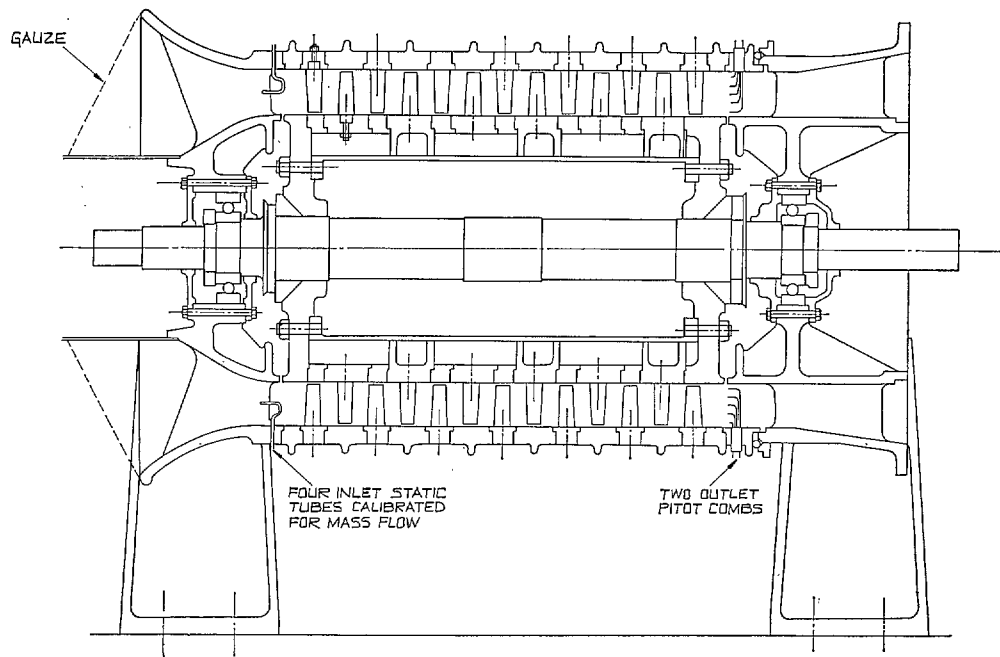


FIG. 1. Assembly of compressor.

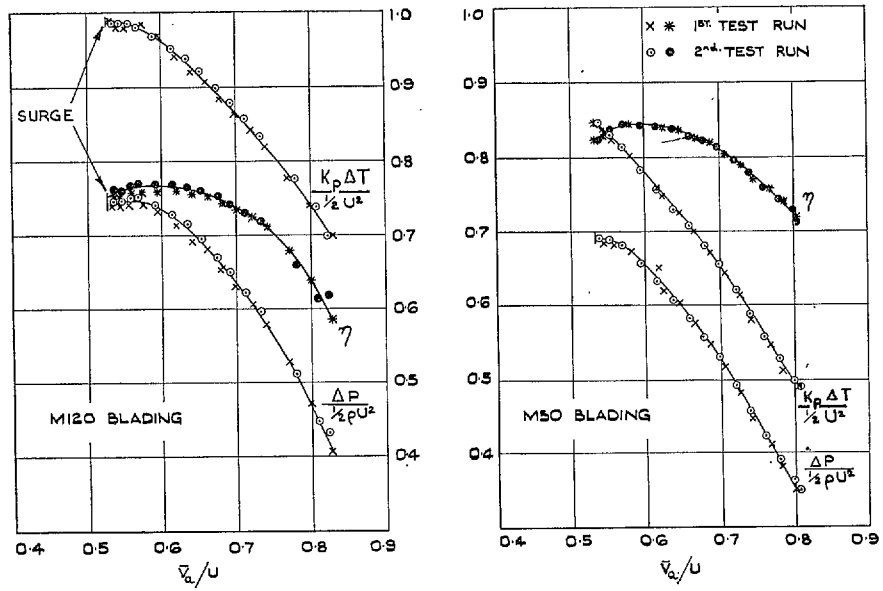


FIG. 2. Overall characteristics, M120 and M50 bladings.

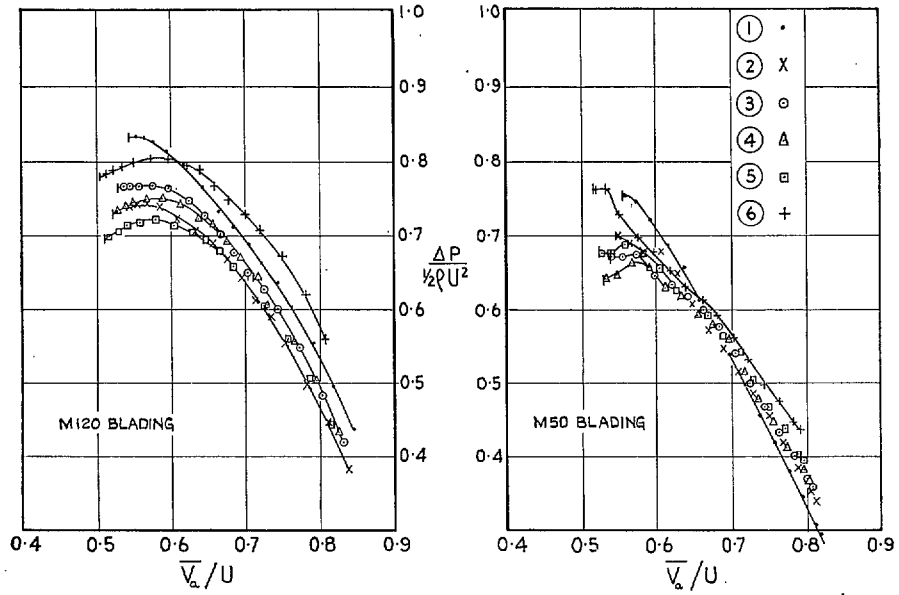


FIG. 3. Stage characteristics. M120 and M50 bladings.

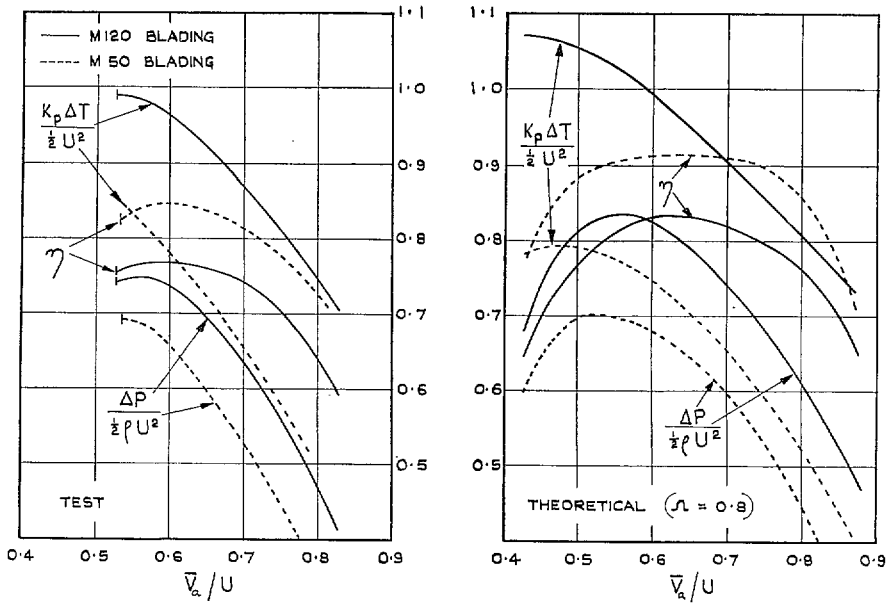


FIG. 4. Test and theoretical overall characteristics compared. M120 and M50 bladings.

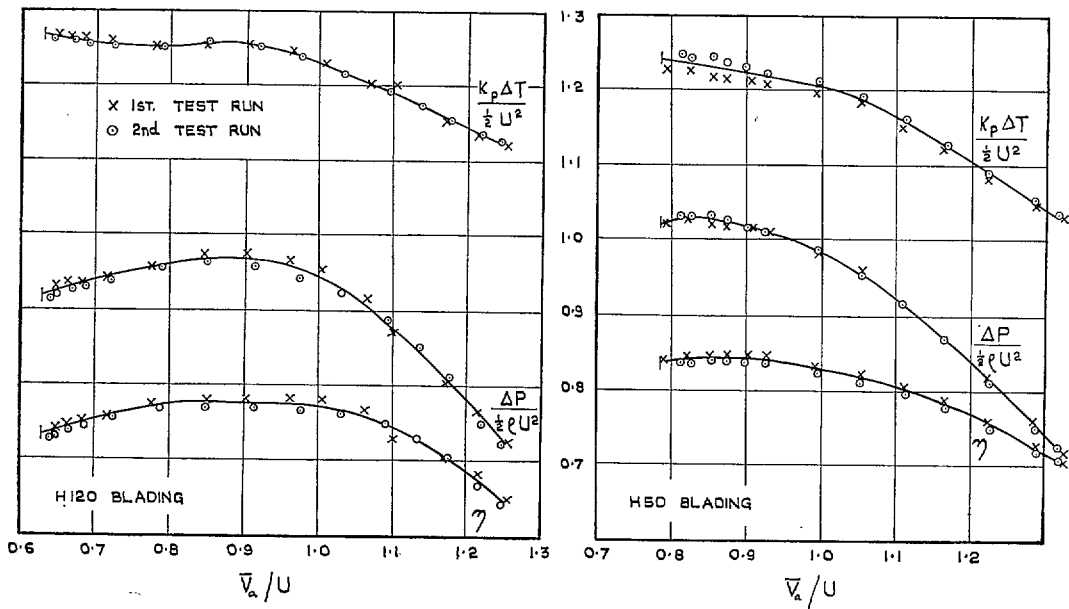


FIG. 5. Overall characteristics. H120 and H50 bladings.

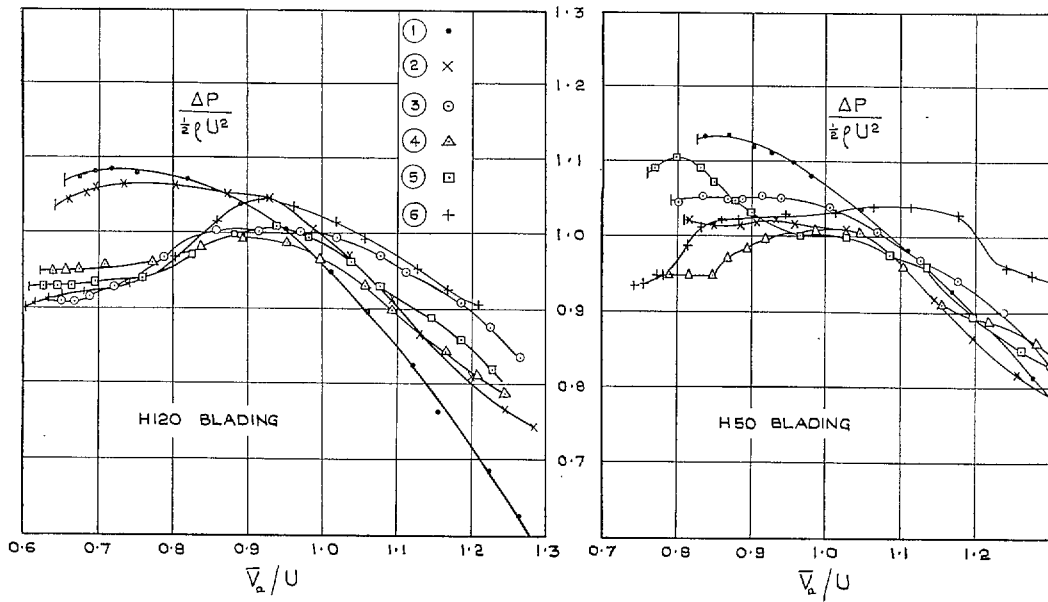


FIG. 6. Stage characteristics. H120 and H50 bladings.

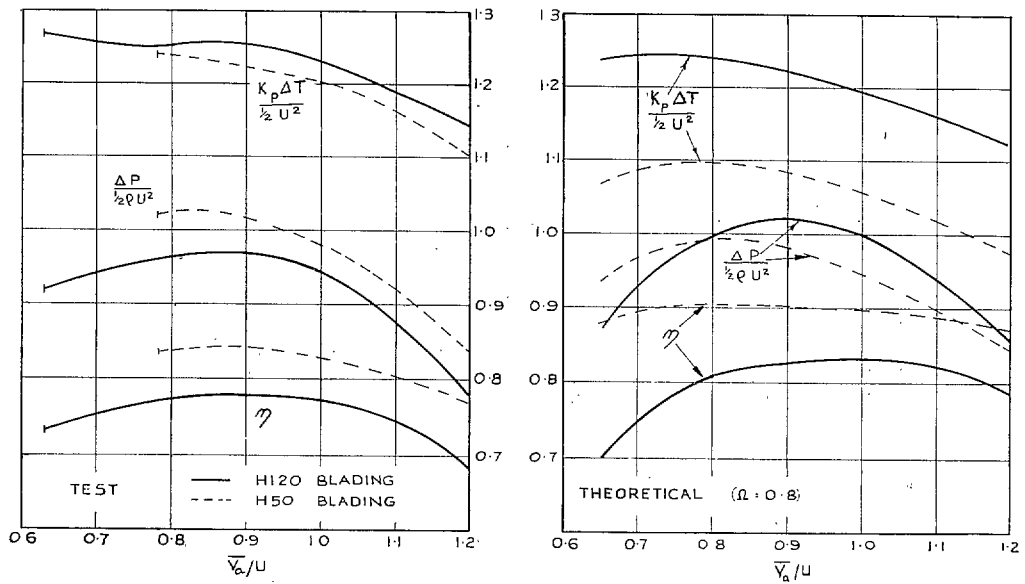


FIG. 7. Test and theoretical overall characteristics compared. H120 and H50 bladings.

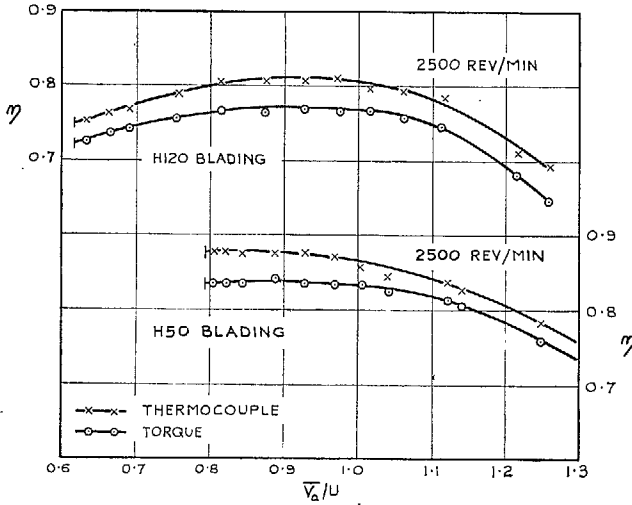
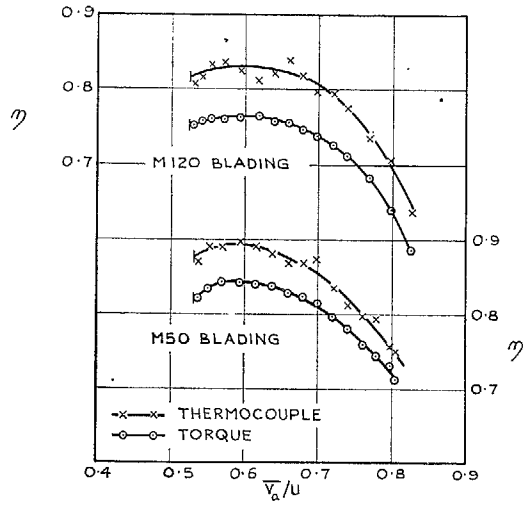


FIG. 8. Comparisons of torque and thermocouple efficiencies. All bladings.

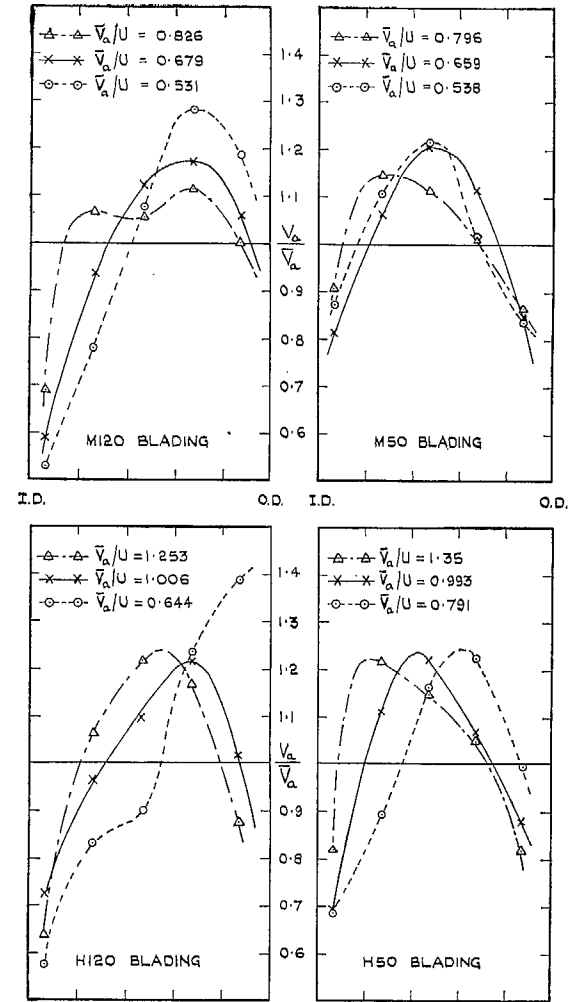


FIG. 9. Outlet-annulus velocity profiles. All bladings.

Publications of the Aeronautical Research Council

ANNUAL TECHNICAL REPORTS OF THE AERONAUTICAL RESEARCH COUNCIL (BOUND VOLUMES)

- 1942 Vol. I. Aero and Hydrodynamics, Aerofoils, Airscrews, Engines. 75s. (post 2s. 9d.)
Vol. II. Noise, Parachutes, Stability and Control, Structures, Vibration, Wind Tunnels. 47s. 6d. (post 2s. 3d.)
- 1943 Vol. I. Aerodynamics, Aerofoils, Airscrews. 80s. (post 2s. 6d.)
Vol. II. Engines, Flutter, Materials, Parachutes, Performance, Stability and Control, Structures. 90s. (post 2s. 9d.)
- 1944 Vol. I. Aero and Hydrodynamics, Aerofoils, Aircraft, Airscrews, Controls. 84s. (post 3s.)
Vol. II. Flutter and Vibration, Materials, Miscellaneous, Navigation, Parachutes, Performance, Plates and Panels, Stability, Structures, Test Equipment, Wind Tunnels. 84s. (post 3s.)
- 1945 Vol. I. Aero and Hydrodynamics, Aerofoils. 130s. (post 3s. 6d.)
Vol. II. Aircraft, Airscrews, Controls. 130s. (post 3s. 6d.)
Vol. III. Flutter and Vibration, Instruments, Miscellaneous, Parachutes, Plates and Panels, Propulsion. 130s. (post 3s. 3d.)
Vol. IV. Stability, Structures, Wind Tunnels, Wind Tunnel Technique. 130s. (post 3s. 3d.)
- 1946 Vol. I. Accidents, Aerodynamics, Aerofoils and Hydrofoils. 168s. (post 3s. 9d.)
Vol. II. Airscrews, Cabin Cooling, Chemical Hazards, Controls, Flames, Flutter, Helicopters, Instruments and Instrumentation, Interference, Jets, Miscellaneous, Parachutes. 168s. (post 3s. 3d.)
Vol. III. Performance, Propulsion, Seaplanes, Stability, Structures, Wind Tunnels. 168s. (post 3s. 6d.)
- 1947 Vol. I. Aerodynamics, Aerofoils, Aircraft. 168s. (post 3s. 9d.)
Vol. II. Airscrews and Rotors, Controls, Flutter, Materials, Miscellaneous, Parachutes, Propulsion, Seaplanes, Stability, Structures, Take-off and Landing. 168s. (post 3s. 9d.)
- 1948 Vol. I. Aerodynamics, Aerofoils, Aircraft, Airscrews, Controls, Flutter and Vibration, Helicopters, Instruments, Propulsion, Seaplane, Stability, Structures, Wind Tunnels. 130s. (post 3s. 3d.)
Vol. II. Aerodynamics, Aerofoils, Aircraft, Airscrews, Controls, Flutter and Vibration, Helicopters, Instruments, Propulsion, Seaplane, Stability, Structures, Wind Tunnels. 110s. (post 3s. 3d.)

Special Volumes

- Vol. I. Aero and Hydrodynamics, Aerofoils, Controls, Flutter, Kites, Parachutes, Performance, Propulsion, Stability. 126s. (post 3s.)
- Vol. II. Aero and Hydrodynamics, Aerofoils, Airscrews, Controls, Flutter, Materials, Miscellaneous, Parachutes, Propulsion, Stability, Structures. 147s. (post 3s.)
- Vol. III. Aero and Hydrodynamics, Aerofoils, Airscrews, Controls, Flutter, Kites, Miscellaneous, Parachutes, Propulsion, Seaplanes, Stability, Structures, Test Equipment. 189s. (post 3s. 9d.)

Reviews of the Aeronautical Research Council

1939-48 3s. (post 6d.)

1949-54 5s. (post 5d.)

Index to all Reports and Memoranda published in the Annual Technical Reports

1909-1947

R. & M. 2600 (out of print)

Indexes to the Reports and Memoranda of the Aeronautical Research Council

Between Nos. 2351-2449

R. & M. No. 2450 2s. (post 3d.)

Between Nos. 2451-2549

R. & M. No. 2550 2s. 6d. (post 3d.)

Between Nos. 2551-2649

R. & M. No. 2650 2s. 6d. (post 3d.)

Between Nos. 2651-2749

R. & M. No. 2750 2s. 6d. (post 3d.)

Between Nos. 2751-2849

R. & M. No. 2850 2s. 6d. (post 3d.)

Between Nos. 2851-2949

R. & M. No. 2950 3s. (post 3d.)

Between Nos. 2951-3049

R. & M. No. 3050 3s. 6d. (post 3d.)

Between Nos. 3051-3149

R. & M. No. 3150 3s. 6d. (post 3d.)

HER MAJESTY'S STATIONERY OFFICE

from the addresses overleaf

© *Crown copyright 1964*

Printed and published by
HER MAJESTY'S STATIONERY OFFICE

To be purchased from
York House, Kingsway, London W.C.2
423 Oxford Street, London W.1
13A Castle Street, Edinburgh 2
109 St. Mary Street, Cardiff
39 King Street, Manchester 2
50 Fairfax Street, Bristol 1
35 Smallbrook, Ringway, Birmingham 5
80 Chichester Street, Belfast 1
or through any bookseller

Printed in England